UNIVERSITY OF BARCELONA AND

UNIVERSITY AUTONOMOUS OF BARCELONA

Reservoir Geology and Geophysics Master's Degree Final Project

TECTONIC STRUCTURE OF THE RIVERA PLATE USING MULTICHANNEL SEISMIC DATA ACQUIRED IN THE WESTERN MEXICAN MARGIN (TSUJAL SURVEY, 2014)

Presented by

Estefanía Górriz Ibáñez

and supervised by

Dr. Rafael Bartolomé (ICM-CSIC) and Dr. David Martí (ICTJA-CSIC)

Barcelona, June 26 2015

ABSTRACT

The western margin of Mexico is considered one of the most active seismic zone in America and the Rivera plate is particularly a region where large earthquakes have occurred with very destructive consequences, including the generation of big tsunamis. Two major earthquakes occurred in the area the last century, a magnitude 8.2 in the Jalisco coast in 1932 and in 1995 a magnitude 8.0 located offshore Jalisco southern area. Considering that the rupture area of the 1995 EQ spans only the southern half region of the 1932 EQ rupture area and that the recurrence time estimated is 77 years, likelihood of a rupture event in the northern half of the area is very high, so the Jalisco Block is a zone of high seismic potential. This work aims to characterize the internal structure of the subduction zone of the Rivera plate beneath the North American plate in order to understand the geodynamic and the recent tectonic deformation occurring in the area to relate with the possible generation of tsunamis and earthquakes. For this purpose, it has been carried out seismic processing and geological interpretation of a seismic profile running perpendicular to the margin, from TSUJAL project (2014), located offshore in the Rivera subduction zone beneath the NorthAmerican Plate.

1. INTRODUCTION

Subduction is a geological process in which one lithospheric plate is being drawn down or overridden by another tectonic plate, along their boundary (subduction zone). The process is in the response to a problem of space during the convergence between the two tectonic plates. When one oceanic plate subducts beneath a continental plate, the time required to be forced below is faster than the time required for the mantle heating up, so the plate stays cooler, denser and mechanically more rigid than the surrounding mantle. This “slab pull” is thought to be response for the movement of tectonic plates across the Earth’s surface. The large friction between the two plates, accumulating large amount of energy, resulting in tensions and faulting in the Earth’s crust, causes major earthquakes (and volcanic eruptions) whose hypocenters are concentrated in the so-called Benioff Zone or seismogenic layer. Some of these hypocenters are located below the ocean floor and when ruptures reach the seafloor can cause the displacement of a large volume of water and the formation of large seismic sea waves or tsunamis. This friction between the two plates also origins partial melting of the mantle, which rises to the surface as magma and leads to a formation of a volcanic belt parallel to the subduction zone, within the Benioff zone.

Subduction zones are very active seismic and volcanic areas and the greater risk occurs in coastal areas where earthquakes and tsunamis suppose a danger to the populations. Therefore, the investigation of subduction zones and seismogenic and volcanic areas associated become extremely important for the safety of people living in these areas. Research in subduction zones includes several geophysical techniques and such multichannel reflection seismic (magnetism, gravity, high resolution

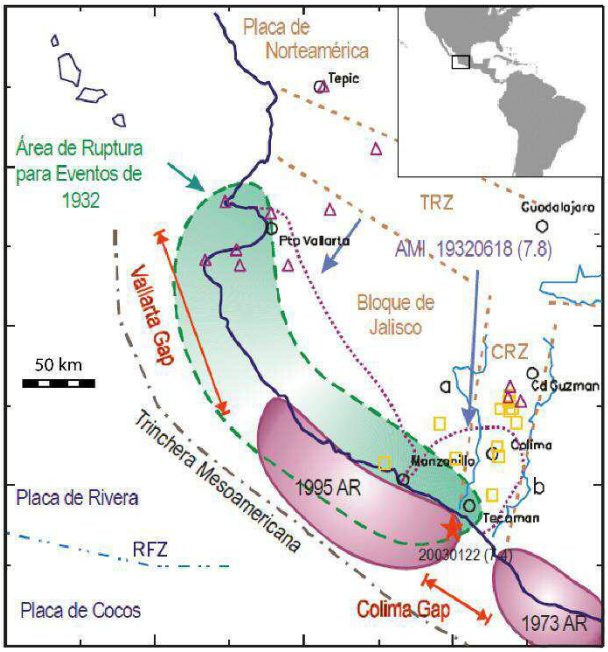

Fig. 1 – Seismotectonic map of the Jalisco block coast, showing the rupture zones of great earthquakes and existing seismic gaps (Image modified from TSUJAL Marine Cruise Report).

bathymetry and geology sampling). The main objective of this work is to characterize the internal structure of the subduction zone to understand the geodynamic and the recent tectonic deformation occurring in the area. This information will be of paramount importance for seismic hazard assessment. For this purpose, this manuscript describes the acquisition, processing and the geological crustal interpretation of a multichannel seismic marine profile.

2. GEOLOGICAL SETTING

The western margin of Mexico is structurally composed by the interaction of several tectonic plates and is considered one of the most active seismic zone in America. It includes the subduction of the Rivera oceanic plate beneath the North America (NA) plate, being the Middle American Plate the morphologic expression of the subduction contact. The seismicity in Mexico along the Middle America Trench has been widely studied (Eissler & McNally, 1984, Singh et al., 1985 and DeMets & Stein, 1990) and is the area where largest earthquakes are located in the recent history of Mexico. Attending to the macroseismic data, 10 large earthquakes have been produced in the last 120 years. The largest historical earthquake occurred on the coast of Jalisco (19ºN) in 1932 (Eissler and McNally, 1984, and Singh et al., 1985), with a magnitude of 8 followed by one aftershock of M_s=7.8 fifteen days after causing 300 deaths, leaving 25 injured and towns severely damaged. This aftershock generated a catastrophic tsunami that wiped out a 25 km stretch of coastline. Its run-up reportedly reached 10 m (Sanchez & Farreras 1993). In 1995 an earthquake with a magnitude of M_s=8 occurred offshore southern Jalisco killing 49 people and thousands of homeless. The quake also triggered a tsunami along the coast of Jalisco and Colima states having a run-up height of 5.1 m that affected a 200 km stretch of coast with severe damage confined to areas with shallow shoreline topography (Figure 1). The rupture area occurred in the 1995 event spans only the southern half of the area affected by the earthquake of 1932. The recurrence time estimated for earthquakes similar to the 1932 on the coast of Jalisco is 77 years (Singh et al, 1985) and considering that the earthquake of 1995 was generated with the rupture of only the southern half of the fractured area in 1932, suggests that the likelihood of a rupture event in the northern half of the area is very high. Geological hazard in the area includes as well three significant volcanoes: Sanganguey, Ceboruco, and the Fire Volcano, the most active volcano in Mexico.

The Rivera Plate is a microplate with an extension of 100000 km^2 (DeMets & Stein, 1990) and it is surrounded by three lithospheric plates: North America, Cocos and Pacific plates. The complex tectonic setting of the Rivera plate can be

divided into two distinct regions. The first one is the Middle American Trench (MAT) (Figure 2), which is located west of Mexican margin around 21° N and it forms the active convergent margin of western Mexico, a collision zone where the Rivera microplate and Cocos plate subducts beneath the North America plate, respectively (Lonsdale, 1989). The convergence rate at the Middle America Trench has fluctuated strongly during the last 10 M.y., but the lithosphere currently entering the subduction zone appears to have formed at a full spreading rate of around 97 mm/yr (DeMets, 2000). Local earthquake data indicate a Benioff zone dipping at around 10º to 20 km depth, then steepening to 50º at 40 km depth (Pardo et al. 1993). The second region is the Tamayo Fracture Zone (TFZ), located in the northern limit, composed by a 70 km long transform fault between the MAT and the southern San Andreas transform fault system, which connects to the south with the accretion zone of the Pacific Rivera Rise (PRR) (Figure 2). The PRR represents the plate boundary between the Rivera and Pacific plates and has a spreading rate of 50 mm/yr (DeMets & Stein, 1990). The Rivera Fracture Zone (RFZ) is an accurately transform fault located to the SW of the Rivera plate and it offsets the southern Pacific-Rivera Rise and northern East-Pacific Rise (EPR) (Figure 2). The EPR represents the accretion of new oceanic crust which forms a boundary between the Cocos and the Pacific plates (Figure 2). Eissler and McNally (1984) suggest that it may be a Rivera – Cocos boundary NE trending, left-lateral strike-slip boundary, connecting the Rivera transform to the MAT. Alternatively, one or more E-W dextral strike-slip faults may connect the northern end of the East-Pacific Rise to the Middle American Trench (Bandy et al., 2000).

The Jalisco Block, located inland in west of Mexico, which is generally considered as part of the North American plate, may have some degree of independent motion. There are active faults along the Tepic-Chapala, Colima and Chapala rifts

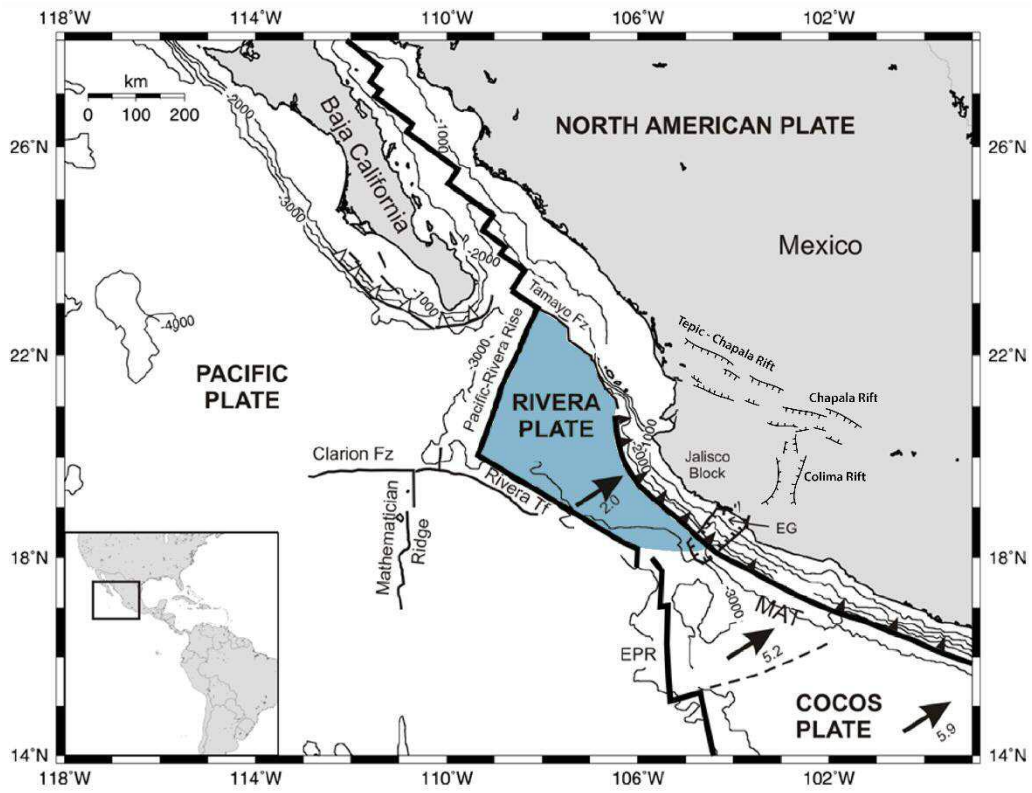

Fig. 2 – Location map of study area showing the major tectonic features: Rivera and Cocos plates subducting beneath the North American plate and transform faults zones associated to spreading. The relative rates of convergence (cm / year) between oceanic and continental plates are indicated by arrows (Pardo et al, 1995). EPR: East Pacific Rise, MAT: Middle America Trench, OFZ, Orozco Fracture Zone; TME: Tres Marias Rise, EG, El Gordo Graben (Image modified from TSUJAL Marine Cruise Report)

in southwestern Mexico that may be related to Rivera - -North America tectonics (Allan, 1986, Johnson and Harrison, 1989, and Allan et al., 1990) (Figure 2).

Moreover, there are large amounts of methane hydrate beneath the seafloor in the accretion wedge. Methane hydrate deposits represent a promising source of energy for the future, but the technology for industrial production is still not available. Recent studies evidence gas hydrates in the West of Mexico (Bartolome et al., 2011; Bandy et al., 2012) in the form of bottom simulating reflectors (BSR) on multichannel seismic reflection profile located in the continental slope area of the northern part of the Jalisco Subduction Zone, off Puerto Vallarta between 20º and 20.5ºN.Thus, there is evidence to suggest that the Pacific margin of Mexico may content significant reserves of hydrocarbons in form of gas hydrates. Exploration of the margin may continue for a full evaluation of this potential. This work go in this direction.

To understand the complex plate interactions, resulting in a wide variety of tectonic processes that produce the exceptional geodynamic setting in the western Mexican margin. The TSUJAL project (*Crustal characterization of the Rivera Plate-Jalisco Block boundary and its implications for seismic and tsunami hazard assessment*) was designed and funded by the Spanish and the Mexican Governments. TSUJAL is a geophysical experiment combining the application of several techniques to acquired marine data offshore in the subduction area of the Rivera Plate beneath NA plate. The global objective of the TSUJAL project is the characterization of the shallow and deep lithospheric structure from the seabed into the upper mantle, and the identification of the geological sources which can trigger earthquakes and tsunamis on the West coast of Mexico.

3. DATA ACQUISITION

During TSUJAL survey, a total of 14 multichannel seismic (MCS), swath-bathymetry, parametric echosounder and gravity profiles were acquired along and across the Rivera subduction zone, the main faults and prominent structures of Mexico. This paper focuses on the multichannel seismic (MCS) marine profile named TS06b, acquired during the TSUJAL survey on the February 28 2014 (Manzanillo, Mexico) on board of the RRS James Cook (NERC, UK) using the digital and solid state streamer of the Unidad de Tecnología Marina (UTM – CSIC, Spain).

The preliminary interpretation of the MCS data before processing allowed us to identify a likely anomalous reflector associated to a polarity change in the seismic signal, commonly named Bottom Simulating Reflector (BSR). TS06b has a

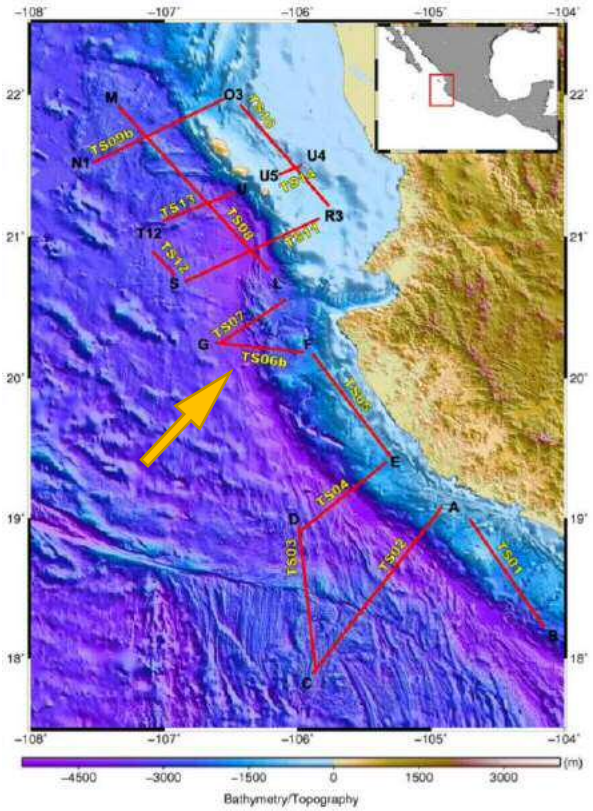

Fig. 3 – Multichannel seismic profiles acquired during TSUJAL survey. The TS06b profile is indicated by an arrow. Position based on the COS location during MCS shooting (Image obtained from TSUJAL Marine Cruise Report)

START OF LINE		END OF LINE	
LAT (º)	LONG (º)	LAT (º)	LONG (º)
20.183	-105.958	20.248	-106.610

Tab. 1 – Location of the multichannel seismic profile TS06b acquired during TSUJAL survey

total length of 65.45 km and an approximate orientation of ESE-WNW (Table 1), running almost perpendicular to the Rivera subduction beneath NA plate (Figure 3).

The source array was designed to maximize the energy concentrated at the lowest frequency range. The shooting interval was defined at 50 m, as a compromise between maximum redundancy of data (CMP fold) and capacity of the air compressors. But a continuous failed of the guns was mostly due to air lines breaks. The best solution for this problems forces to change big guns to medium-small volume chambers, decreasing the total volume of the gun array. The design of the new source was done again using Gundalf® commercial software (Table 2).

The arrays towed off from the center of the stern at port and starboard sides getting a symmetrical

SOURCE PARAMETERS AND CONFIGURATION	
Total number of guns	12 (3 guns for array)
Source controller	Big Shot ®
Source type	Bolt® G.Guns 1500LL
Compressors	4 x Hamworthy® 4TH 565 W100
Air pressure	2000 psi
Maximum spectral value (db): 10.0 - 50.0 Hz.	212
Average spectral value (db): 10.0 - 50.0 Hz.	210
Total acoustic energy	164659.5 (Joules)
Total volume	3540 cu.in (58 liters)
Maximum volume supplied	675 m³/h (400 cfm)
Number of arrays	4
Gun synchronization	+/- 0.1 ms
Deployment depth	8 m
Shot interval	50 m
Aiming point	50 ms
Separation between guns	2.8 m between plates
Inner arrays	Located at 11 m from the center of source

Table 2 – Details of seismic source used during acquisition of profile TS06b

STREAMER PARAMETERS	
Streamer model	SSAS Multichannel Sentinel Sercel®
No. of hydrophones per channel	8
Depth	10 m
Active channels	468
Active length	5850 m
Near offset	137.8 m
Group interval	12.5 m
Last channel – Tailbuoy	82.1 m
No. compasses	19
No. bird	16
CMP distance	6.25
CMP nominal fold	58 – 59
Auxiliary channels	6

Table 3 – General acquisition streamer parameters defining profile TS06b

configuration from the streamer. The main purpose of mixing different volume guns is improving signal characteristics because it increases the power of the source and will have different bubble periods, leading to a constructive summation of the primary peak and destructive summation of the bubble (secondary peaks) amplitudes (Figure 4).

Shooting during the cruise was carefully carried out following established rules to avoid harm of local marine mammals, using soft starts and monitoring the presence of marine mammals and turtles in the vicinity of the vessel, which caused to stop shooting repeatedly.

The receivers used during the acquisition of profiles was a 5.85 kilometers-long Sercel SEAL streamer with a total of 468 channels (39 active sections of 12 active channels) (Table 3).

4. SEISMIC REFLECTION PROCESSING

The main objective of seismic processing is to produce an interpretable image using redundant reflection seismic records, or section in 2D acquisition, that represents the geological structure below the surface. To obtain seismic images, several processing must be applied to the seismic

data to improve the seismic resolution and to increase the signal \ noise ratio.

The main applied processing steps include: I) prestack signal enhancement (editing traces and filtering), II) deconvolution, to improve vertical resolution, III) velocity analysis every 200 CMP, IV) Radon demultiple, to suppress multiple seafloor arrivals, V) NMO correction and stack to which increases the signal/noise ratio, and, finally, V) migration, which increase the horizontal resolution and collapse diffractions re-locating in time the events. Time variant band-pass filtering and gain have been applied for final imaging.

4.1 Processing steps

The processing of the TS06b seismic line was carried out using the software package Globe Claritas due to the availability of licenses in CSIC. I applied a standard processing working flow for multichannel marine seismic data (Figure 5), defining and designing very carefully the specific parameters for every step, as required by the quality of data. I will concentrate my efforts highlighting the description of some of the processing steps within this section.

4.1.1 Geometry definition

The real marine geometry has been calculated and added into the trace headers (see figure 5), using the original positioning information obtained from navigation files, which includes: hydrophone and source GPS positions, channel number and shot identification number. This information is critical in the processing work, and also for the CMP calculation (Table 4).

RESULTING GEOMETRY	
Shot range	101 – 1410
CDP interval	6.25
Nominal fold	59
Max. fold	63
CDP range	100 - 11159

Table 4 – Detailed information of resulting geometry

4.1.2 Prestack processing

The aim of this processing step is to improve the signal /noise ratio of the recorded data (see figure 5). To achieve this objective two main processes have been applied to the raw data in the shot domain: trace editing and muting. The trace editing lies in identifying and deleting all the noisy traces existing in the shot gathers. Edited traces can be single traces that become noisy for channels (hydrophones) within the streamer that systematically shows a malfunction during the acquisition. This is the case for channels 252 and 260 in TS06b, were deleted for all the shot gathers (Figure 6). Furthermore, water layer signals (direct wave) have been removed as well as the first arrivals corresponding to refractions shot by shot.

During the TSUJAL survey the JNCC Rules (Joint Nature Conservation Committee), the public body that advises the UK Government and administrations on UK in nature conservation programs have been observed. Thus, shooting airguns was carefully carried out following established rules to avoid harm of local marine

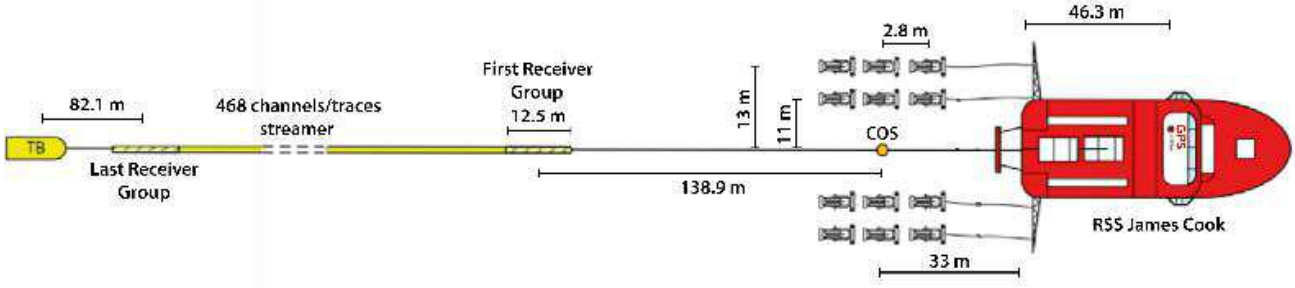

Fig. 4 – Gun array and streamer configuration used during acquisition of line TS06b (Image modified from TSUJAL Marine Cruise Report)

mammals, using soft starts and monitoring the presence of marine mammals and turtles in the vicinity of the vessel. This procedure caused stop shooting repeatedly. Several gap shooting appears in the seismic section due to turtle sighting during the acquisition of TS06b seismic line and all this traces were replaced for traces with amplitude zero (Table 5). This can be clearly observed performing a *trace near* profile (Figure 7) in which only one trace of every shot is plotted. This profile gives a first approximation of what will be our seismic section, and all the shooting. Furthermore, I used the near trace profile to check misfired air delays during the seismic survey acquisition, which is easily detected as a delay in time respect to the adjacent traces.

SHOTS	STOP TIME
398 - 407	18:41 h
534 - 546	19:30 h
577 - 588	19:46 h
777 - 795	20:57 h
844 - 876	21:22 h
899 - 914	22:08 h
928 - 941	22:18 h

Table 5 – Shot gaps due to turtle and mammal sighting during the TS06b profile acquisition

Prestack also includes a band-pass butterworth filter to the data (see figure 5) to remove low frequency noise and avoid anti-aliasing (see figure 6). The filter was defined by 4 different frequencies, and the high frequencies varies according to the shots location along the profile. The frequencies used for each shot are collected in Table 6.

SHOT	FREQUENCY RANGE (Hz)
101 - 200	4 – 7 – 75 – 90
201 - 300	4 – 7 – 75 – 85
301 - 450	4 – 7 – 75 – 90
451 - 500	4 – 7 – 70 – 85
501 - 550	4 – 7 – 75 – 85
551 - 700	4 – 7 – 70 – 85
701 - 750	4 – 7 – 75 – 85
751 - 950	4 – 7 – 75 – 95
951 - 1410	4 – 7 – 70 – 85

Table 6 – Frequency range used to apply the band-pass filter.

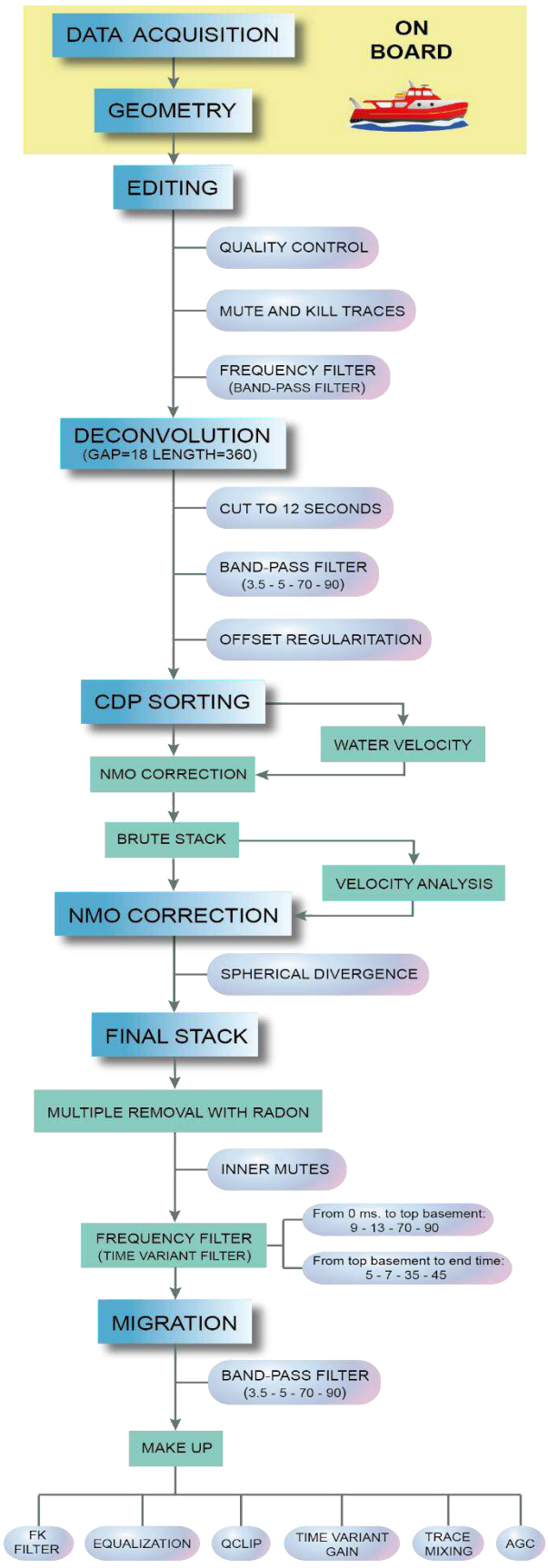

Fig. 5 –Flow processing diagram applied to line TS06b.

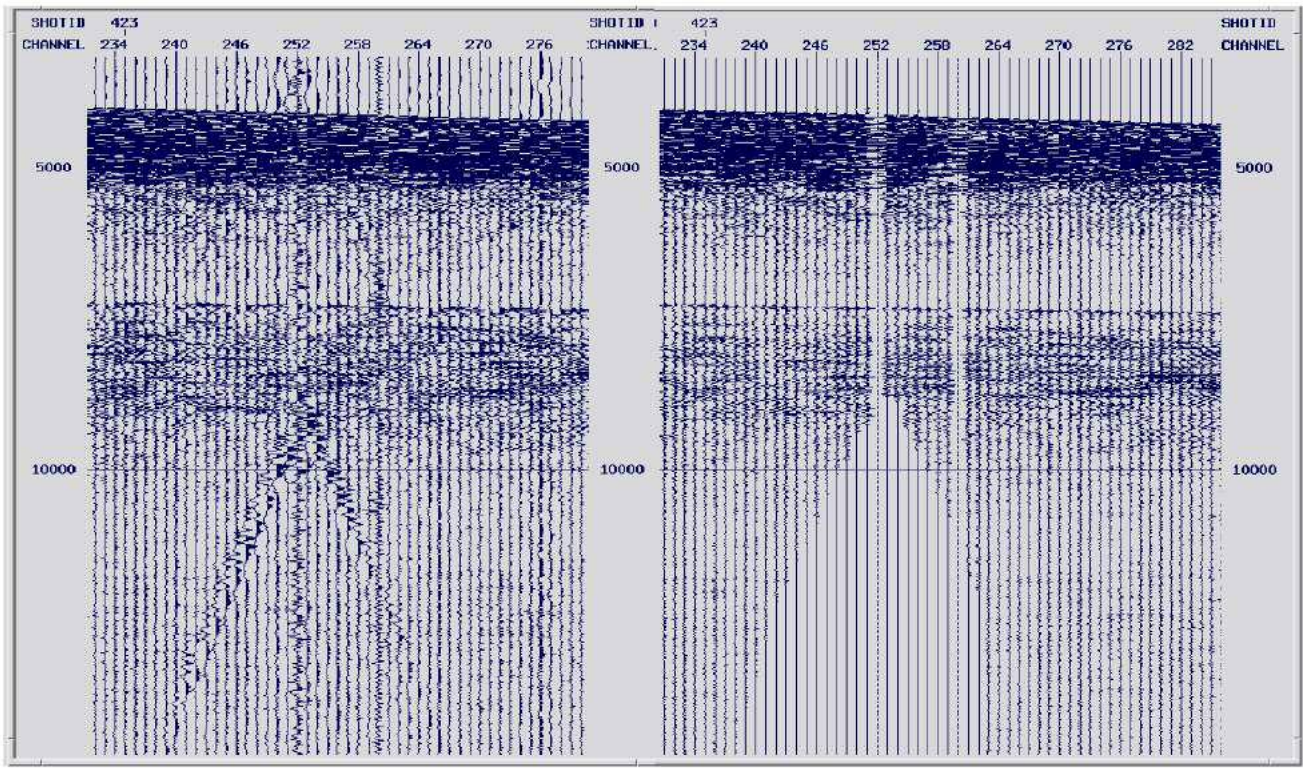

Fig. 6 – Zoom of the shot-gather nº 423 between channels 232 and 280, before (left) and after (right) of the editing and band-pass filter. Vertical scale TWTT (ms).

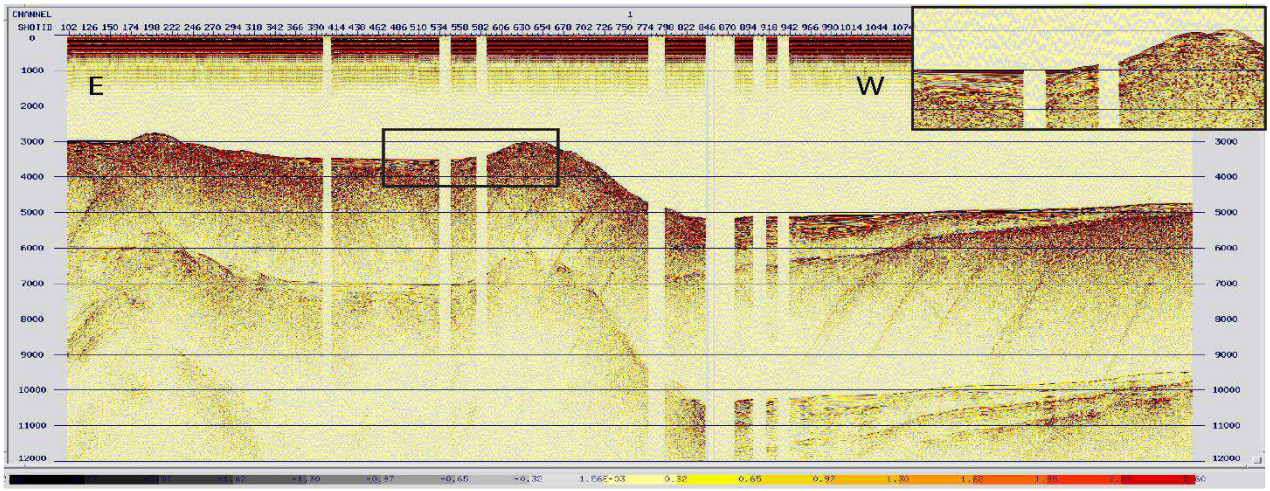

Fig. 7 –Near trace profile with the shot gaps in areas with turtles and mammals sighting. Vertical scale TWTT (ms).

4.1.3 Deconvolution

The aim of the deconvolution is to remove the effects both of the source and the medium through which seismic waves propagate, in order to recover the response of the Earth in the temporal signal recorded (Figures 5 and 8). Thus, deconvolution attenuates the reverberations and short - period multiples, which increases the temporal resolution and impedance contrasts between layers (Yilmaz, 1987). To achieve this, we try to collapse the signal generated in a single pulse, which by interacting

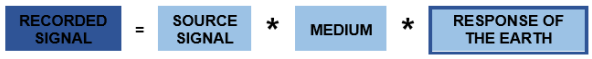

Fig. 8 – Recorded seismic trace in terms of convolution.

with the reflectivity series of the subsurface, giving us the reflectivity function without interference of the wave generated.

A predictive Wiener deconvolution filter was designed defining the optimum gap and length operator parameters to determine the source wavelet. Gap is a time interval of the source wavelet that is associated with the response of the Earth, and the operator length is the total length of the wavelet (Figure 9). After several tests, the best resolution was obtained for a gap of 18 ms. and an operator length of 360 ms (Figure 10B).

After applying the deconvolution, a band-pass filter post deconvolution was applied with a frequency range of 3.5 – 5 - 70 - 90 to eliminate noise generated during deconvolution (see figure 5). In addition, the record length was reduced to 12 seconds because no significant seismic signal has observed beyond this time.

Seismic datasets are generally irregularly sampled in inline midpoint, cross-line midpoints, offset (distance between a hydrophone and its source) and azimuth. This irregular sampling can limit the effectiveness of high resolution on the

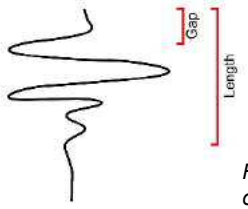

Fig. 9 – Gap and operator length of the source wavelet.

seismic profile. To overcome this issue, I had done an offset regularization (see figure 5). This process transfers samples from their irregular recorded location to locations on a regular grid.

4.1.4 Velocity analysis and NMO correction

Next step in processing consist on sorting the seismic traces according to CDP headers (see figure 5). This consist in gathering traces that, by geometry, belong to the same midpoint between a source and a given receiver (Figure 10A and 10B).

The reflection observed in this CDP gathers are hyperbolic trajectories because they correspond to different offsets. All the information contained in the traces of one CDP is basically the same, so I need to find the hyperbolic corrections that will put every reflection at the same time to add, or stack, them in order to increase the signal to noise ratio. Primary reflections will be highlighted and coherent signals as well if the corrected CDP traces are summed up,

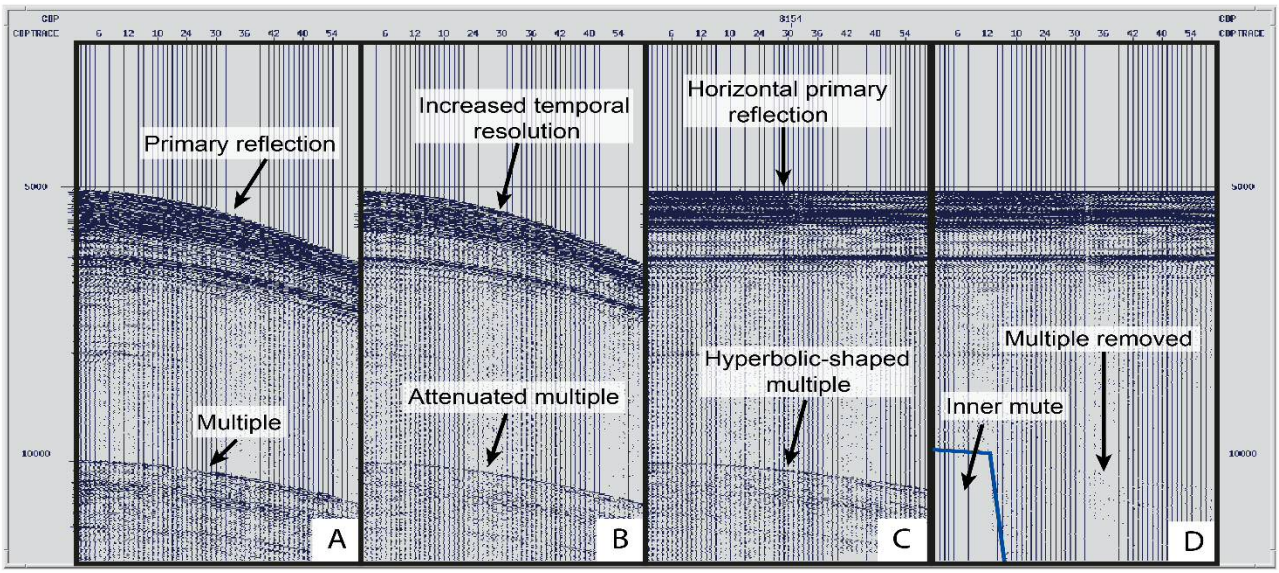

Fig. 10 – Example of corrections applied in the CDP 8154. A) Original CDP. B) CDP with deconvolution and band-pass filter applied. C) CDP with NMO correction. D) CDP with removed multiples. Vertical scale TWTT (ms).

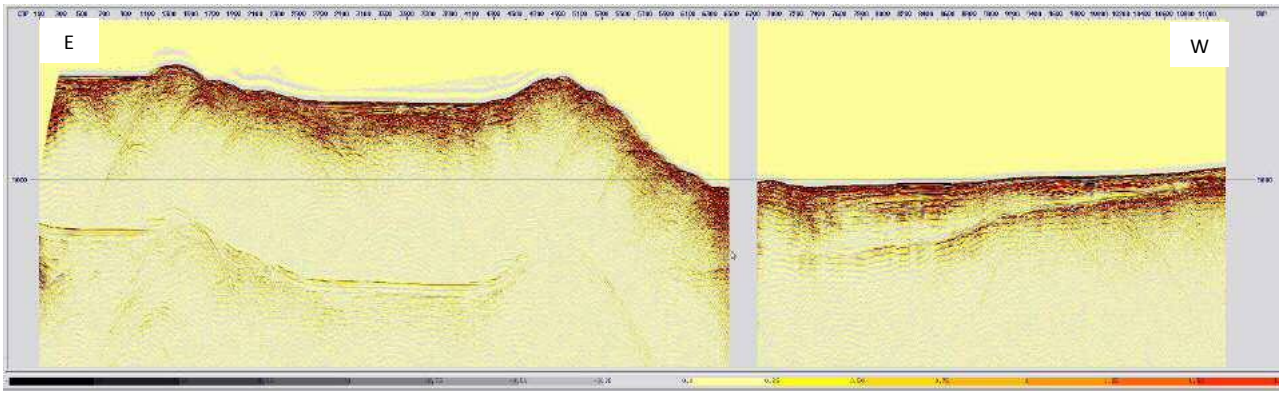

Fig. 11 – Brute stack using water velocity (1500 m / s). I used this profile to perform a RMS velocity model based on the interval velocities. Can be observed the main reflectors but it is difficult to identify structures and stratigraphic relations. Vertical scale TWTT (ms).

and incoherent signal, including noise, direct waves or multiples, will be attenuated. This step is known as NMO correction (Normal Move Out correction) (Figures 5 and 10C). In practice, the way of achieving such alignment is carrying out a RMS velocity analysis (Root Mean Squared). The RMS - velocity is the optimal velocity for which the hyperbola of reflection becomes horizontal in a given time, but does not have to belong to any particular layer.

To obtain a good velocity analysis, I did a brute stack to have a first approximation profile (Figure 11). To obtain the brute stack I used a very simple velocity model based on the water velocity (1500 m/s) without lateral variations or depth (see figure 5). The purpose of the brute stack is to use an initial stack where RMS velocity will be modify to enhance the main primary reflections and improve their lateral continuity.

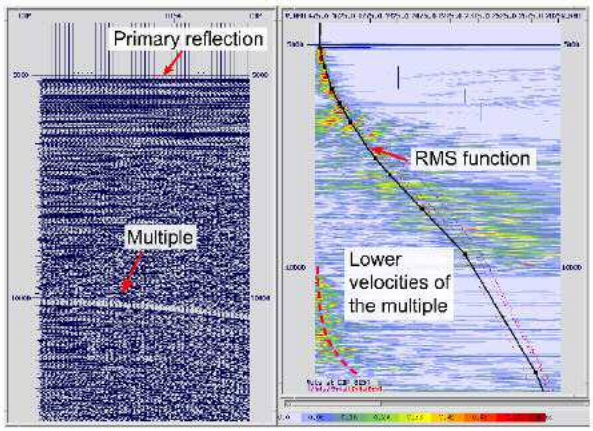

Fig. 12 – Semblance analysis for CDP 8154. Multiple (dotted line) begins to double time that primary reflection and has the same velocity (lower than would correspond to a primary reflection at that depth). Horizontal scale of the CDP is the velocity in m/s and vertical scale is TWTT (ms).

I have used the semblance method for this analysis using the Claritas Velocity Analysis interactive application (CVA) picking velocities every 200 CDPs (Figure 12). The semblance method is based on cross-correlation traces in a CMP gather. Thus, for the same CMP, the stack is calculated for each velocity within a velocity range, which will be the minimum and maximum necessary RMS velocity to flatten the hyperbolas. Therefore the purpose of the velocity analysis is the obtaining of peaks that correspond to the best coherence of the signal in the hyperbolic trajectory throughout the CDP gather. The velocity spectrum allows to distinguish between primary and multiple reflections, because multiples show coherence for lower velocities that expected for a reflection (Figure 12).

On the other hand, the velocity profile resulting from the semblance method is used to apply spherical divergence correction to the data to reconstruct, based on the RMS – velocity corresponding to each point in depth, the lost amplitudes due to absorption of materials and wavefront decaying with distance (see figure 5).

4.1.5 Stack

The RMS velocity model resulting in the previous step allows us to apply the NMO corrections to the CDP gathers and stack the corrected CDP traces (see figure 5). All the reflections are highlighted and the random noise interferences diminishes in a destructive way. The resulting stacked section shows an image in time domain in which the signal/noise ratio has been drastically improved.

The obtained stack profile is not the final section yet because we have to improve the signal attenuating multiple reflections (see Figure 5). The attenuation of multiple reflections in marine seismic data is a high priority in seismic industry for many years. In the case of this profile, the strongest multiple corresponds to the seafloor. This multiple reflection is due to the water – air discontinuity, generated when the energy reflected in the water-air discontinuity surface travels back and another part is again reflected to the seafloor producing a second reflection. That is recorded again by the hydrophones with a double (or triple, if three reflections occurs) time with respect to the first arrival (Figure 13). The multiple is not always easy to eliminate because it can overlap desired primary reflections.

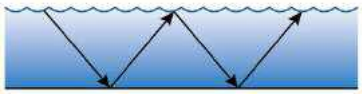

Fig. 13 – Wave reflected twice on the seafloor generating a multiple.

The attenuation of multiple reflections has been performed by the Radon method, which transforms seismic data into a frequency domain where multiples and primaries are distinguishable and can be separated. Algorithms of radon filter relay on NMO correction to discriminate and remove multiples from primaries. Velocities must be picked during the velocity analysis with enough accuracy

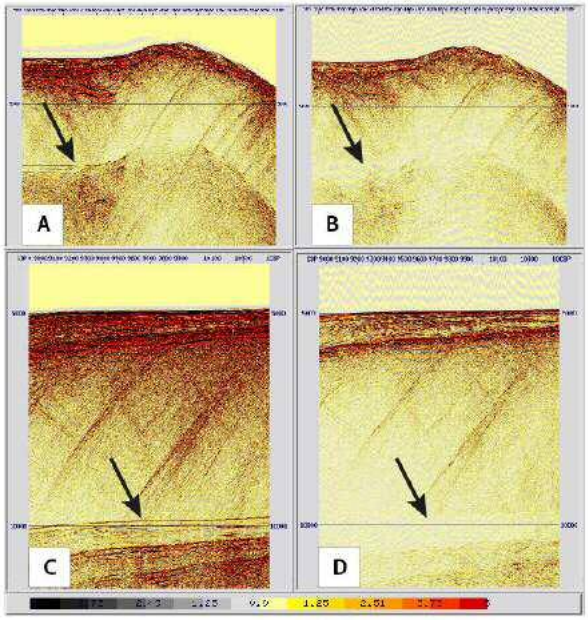

Fig. 14 – Zooms of the Stack. Figures A and B show the before and after applying the Radon to remove multiples between CDP 3500 and 5800. Figures C and D show the before and after between CDP 9000 and 10500. Vertical scale TWTT (ms).

to distinguish primary energy from slightly slower multiple energy (Kumar, 2008). Once applied the Radon method, I performed an inner mute on the internal traces of the CDP gathers (Figure 10D) to remove the portion of the multiple remained. This effect usually occurs when the reflection multiple is horizontal (near offsets) and therefore multiple arrivals may be confused with primary reflections. The multiple attenuation results in a great improvement on the final seismic stacked image, increasing the resolution and reducing the observed noise in previous steps (Figure 14).

To reduce the remnant noise observed in the stacked section, a time- variant band – pass filter was applied at the high- and low- frequency end of the signal spectrum (see figure 5). From 0 ms. to top basement was applied a frequency range of 9 – 13 – 70 – 90 Hz, and from top basement to the end 5 – 7 – 35 – 45 Hz.

4.1.6 Migration

Seismic migration improve the horizontal resolution by collapsing diffractions and moving dipping reflectors to their true position to enhance the spatial resolution and to obtain geologically interpretable stacked section.

Time migration is needed when the stacked section contains diffractions and structural dips, and is suitable for vertically varying velocity and for smooth lateral velocity variations (Yilmaz, 1987), which is the case of the line TS06b. From the different existing migration algorithms, I applied the Finite Difference Time migration (see figure 5). This migration technique is based on a *t-x* domain implicit 45 degree migration, but despite the 45-degree algorithm this method gives reasonable results up to about a 60 degree dip, ideal for our case. The velocity field, which vary in time and space, was defined by the interval velocities model, which was obtained from smoothing and conversion of the RMS velocity model.

With this velocity field, several test were made in some panels, varying the Theta Factor (corresponding to the cosine of the cut off angle) and the Scalar Factor (to define a time-varying velocity scaling). The best results were obtained with a Theta of 0.9 and a Scalar of 1.4, so the Finite Difference migration was applied to entire profile with these parameters (Fig. 15).

4.1.7 Make up

In order to provide the best final seismic section for geological interpretation, a final make-up step has been applied to the data which better define the section obtained at the end of the processing flow. The make-up enhances the image contrast and emphasize, highlight and better define the reflectors. To achieve this result in line TS06b, the following filters and processes have been implemented (see figure 5).

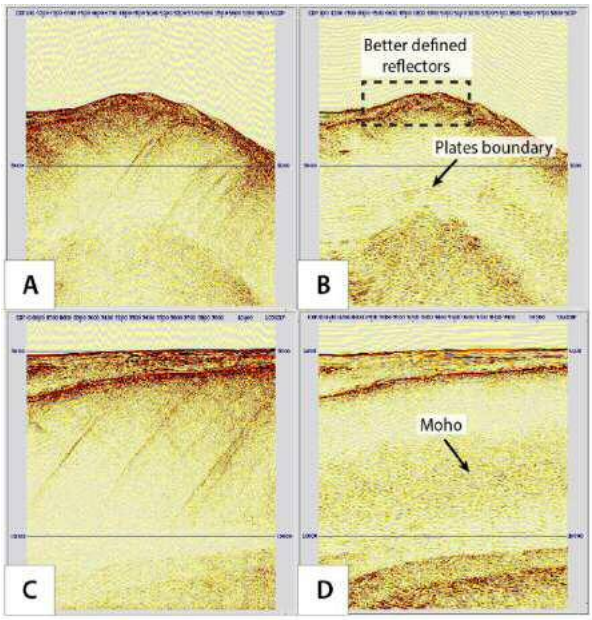

Fig. 15 – Zooms of the Stack. Figures A and B show the before and after applying the Finite differences Time Migration between CDP 1100 and 5900. Figures C and D show the before and after between CDP 8500 and 10300. It can be seen the improvement of the internal structure of the layers by applying the migration. Vertical scale TWTT (ms).

4.1.7.1 F-K Filter

The post-stack F-K Filter provides the muting functions to mute the F-K spectrum of the multiples. This is intended to highlight the Moho reflector, which is within the area of multiple.

4.1.7.2 Equalization

Equalize the trace amplitude applying a user-specified scaling function allows to balance the RMS values of the data traces to a constant specified RMS level.

4.1.7.3 Qclip

The Qclip step is used to remove high-amplitude sample values from the seismic line and replace them with acceptable sample amplitudes. In this case, values outside of 2% are replaced by the threshold value.

4.1.7.4 Time-Variant Gain

The Time-Variant Gain is commonly used to compensate the decaying amplitudes with time by multiplying the data by a gain function. After perform several tests, a gain of time squared was applied.

4.1.7.5 Trace Mixing

The trace mixing computes weighted moving average of the amplitude on a panel of seismic data to enhance the lateral continuity of the reflectors.

4.1.7.6 Automatic Gain Control

The Automatic Gain Control (AGC) is a scaling process which is used for the uniform balancing sets of live traces. Each sample of a trace is multiplied by a scaling calculated factor so that the average amplitude over the given time window length is constant down the trace. The given time window for the line TS06b is 3000 ms.

Once applied the pre-stack, stack and post-stack steps, including the make-up, the resulting seismic section of the line TS06b is ready for geological interpretation (Fig. 16).

4.2 Hydrocarbon occurrence in the western margin of Mexico

Advances in data acquisition and processing now make possible, using seismic traces acquired using multichannel seismic methods, to reveal the presence of hydrocarbons. The changes in the seismic pulses reflected can help to find out the fluids contained within the pore spaces, in particular, the presence of gas. In this way, several hydrocarbons indicators have been identified in the seismic profile TS06b.

First, a prominent identifiable high amplitude bottom simulating reflectors (BSR) has been detected in the accretionary wedge. The presence of BSR is frequently related to the presence of gas hydrates in the marine sediments, although gas hydrates have also been encountered in regions without BSR (Haacke et al., 2007). The BSR imaged, cross-cuttings sedimentary layers, is a reversed-polarity reflectors easily detectable and subparallel to the seafloor. This reflector could be interpreted as a marker for the boundary (as acoustic interference) between sediments containing gas hydrated above (which increases seismic velocity) and free gas below (which lower seismic velocity) in the pore space of accreted sediments (Figure 18A and 18C). Most of the reflection amplitude is caused by the underlying free gas, and therefore, the reduction of the seismic velocity. Whereas gas hydrate can occur without a BSR.

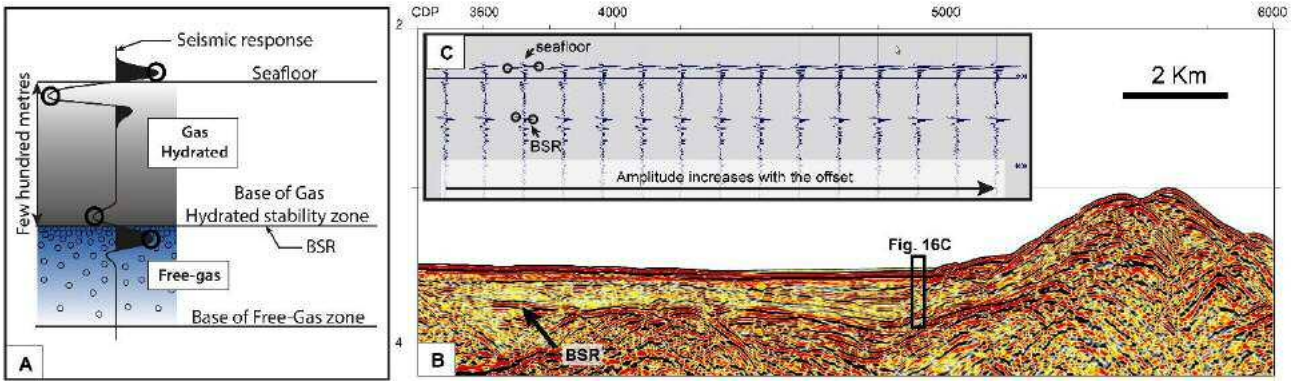

Fig. 18 – Gas hydrate indicator occurrence in the line TS06b. A) Illustration of a submarine section containing the structure and location of gas hydrate (above) and free gas (below) the bottom - simulating reflector (BSR) (Image modified from Haacke et al., 2007). B) Detailed of the accretionary wedge in the seismic profile TS06b showing a clear BSR at 200 -300 m below the seafloor. C) Traces of the CDP 4450 showing a reverse polarity inversion and the amplitude increasing along offset.

Second, there is a geophysical technique called Amplitude Versus Offset (AVO) that can delineate zones of gas, oil and water with a volumetric coverage of surface seismic. This technique is based on the amplitude variation with the offset, i.e. the amplitudes increase, decrease or remain constant with changing angle of incidence, which depends on the nature pore fluid (Chiburis et al., 1993). The long streamer used during the MCS acquisition along the TSUJAL survey has allowed identifying both the BSR and the negative polarity signal at the top of the gas in the section TS06b, becoming more negative when increasing the offset (distance between source and hydrophone) (Figure 18B and 18C).

5 RESULTS

The interpretation of line TS06b contains the primary crustal structure of the oceanic and continental plate. Therefore, the objectives pursued by the seismic processing was focused on obtaining the best image at crustal scale. Taking into account that the airgun source for data acquisition was performed to highlight the main crustal features, the interpretation of the line TS06b follows the same crustal scale motivation, including some local details.

Keeping in mind that I processed a single 2D seismic marine profile, without the integration of other seismic lines acquired in the same area, finally I decided to use the Adobe Illustrator Software Package to elucidate the geological interpretation, rather than the originally planned The Kingdom Suite Software Package, mainly devoted for 3D interpretation.

5.1 General description of the profile

The geodynamic and tectonic involved in the area imaged by the seismic profile TS06b is integrated within the main system of subduction processes of the oceanic Rivera plate beneath the North America plate, extending from the mouth of the Gulf of California to southern of Jalisco block. It can be distinguished in the profile two large areas with different tecto-sedimentary features. The western area (from CDP 7000 to CDP 11000), formed by the subducting oceanic Rivera Plate and sedimentary marine deposits above it. The eastern area (from CDP 100 to CDP 7000), formed by the accretionary prism and the associated sedimentary basins belonging part of the North American Plate. Both areas are delimited by the reflector which marks the limit between tectonic plates, the interplate boundary that we can follow almost continuos all along the profile (Fig. 17). In some zones it has established the crust - mantle boundary (between 7 and 8 seconds two way travel time), which presents discontinuity along the profile and a parallel geometry to the plate boundary, i.e. the top of the Rivera plate (Fig. 17).

The Rivera Plate reflectors imaged indicate that the plate is entering at a gentle dipping, distinguishing a discontinuous crust laterally due to normal faulting process, and horst and grabens as a result of the bow of the plate produced by a bend faulting during subduction (see from km 0 to km 25 in figure 17). Further to the East of the Middle American Trench (around CDP 6700), the top of oceanic basement may be traced continuously for about 20 km beneath the accretionary wedge, and the Rivera plate is covered by about 3 seconds two way travel time (TWTT) of sediments. A pull-up of the Rivera plate under the accretionary prism (from CDP 4000 to CDP 6000) (see figure 17) is observed. This pull-up image effect is caused by the seismic velocity differences during the wave propagation between water column and

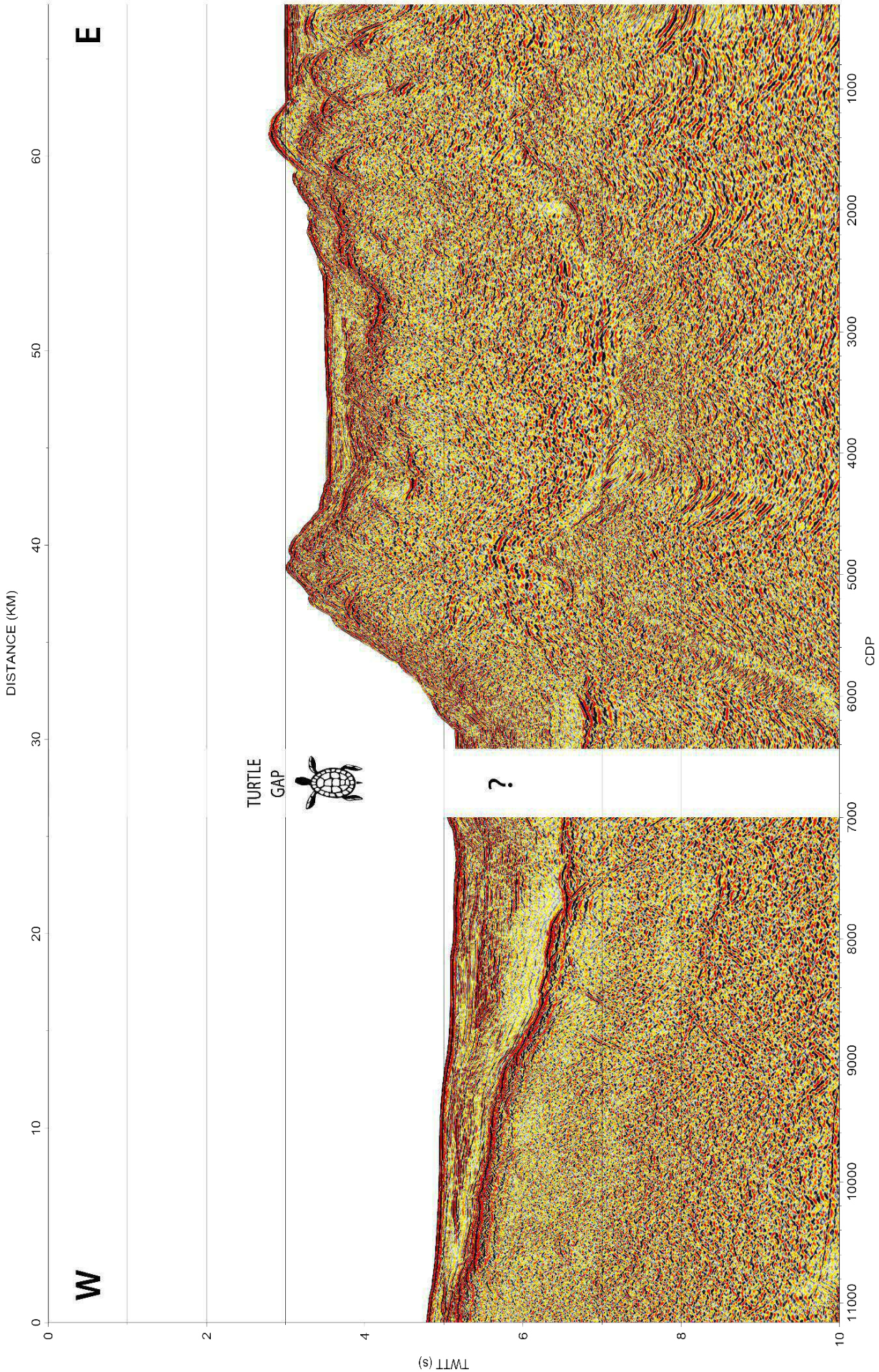

Fig. 16 – Line TS06b processed, cut at 10 at 10 seconds. Vertical scale TWTT (ms).

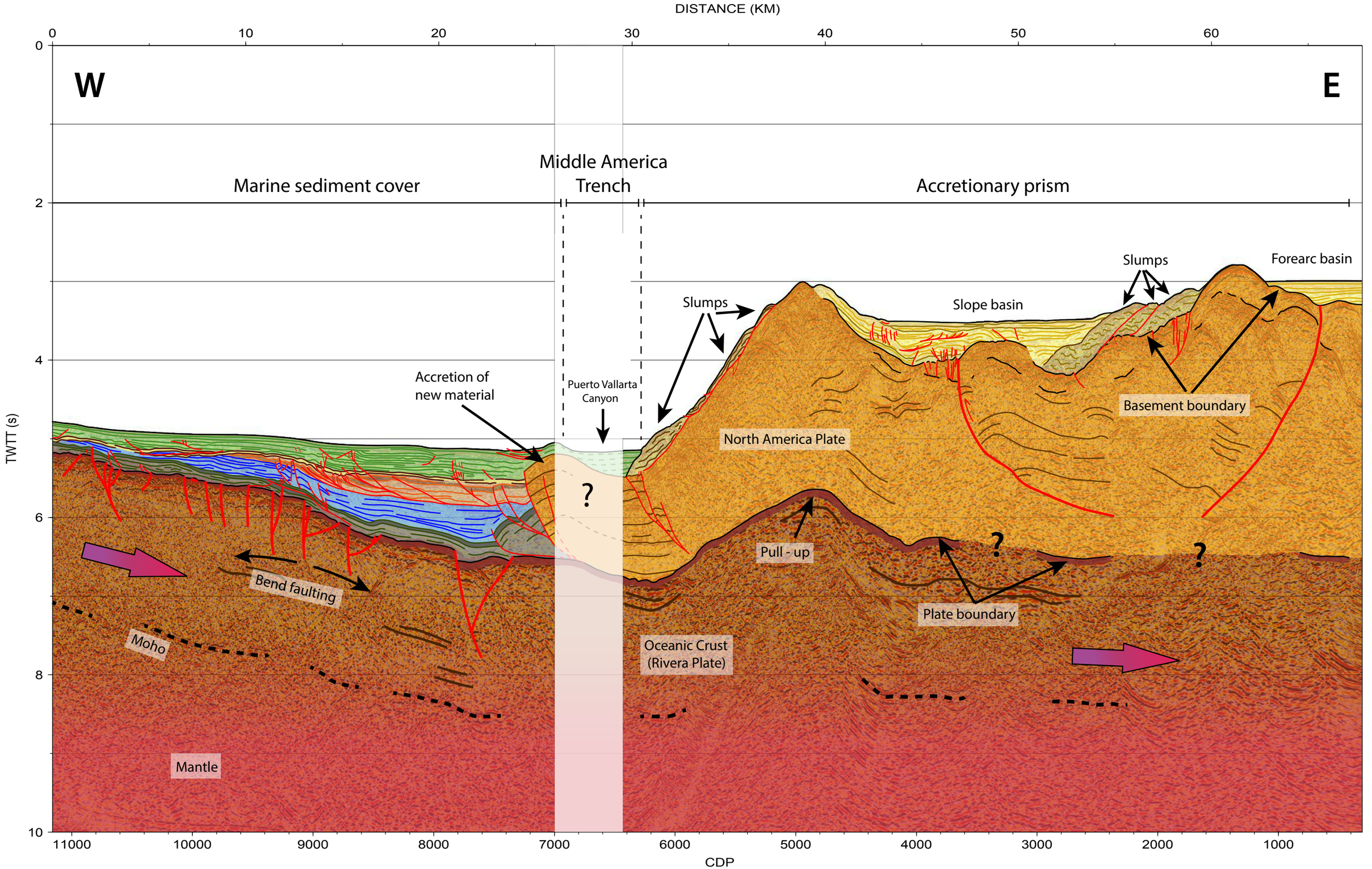

Fig. 17 – Structural interpretation of the line TS06b, where the main structural features can be observed.

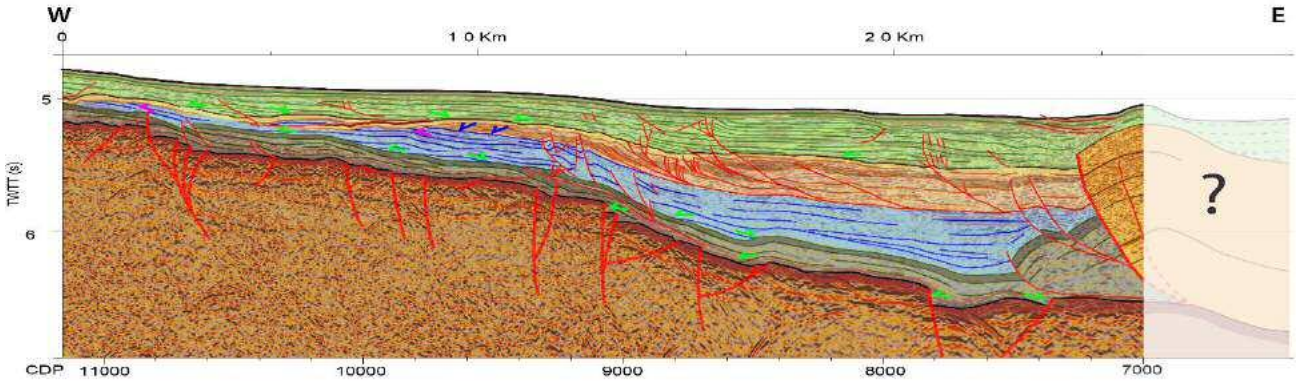

Fig. 18 – Rivera Plate marine sediments units' interpretation. We observe onlap (green arrows), downlap (blue arrows) and erosional truncations (pink arrows) geometries. See the top of the crust faulted due to the bending of the plate when subducting.

accretionary prism and their consequent representation in TWTT.

The sedimentary units located on top of the Rivera plate have strong reflectivity, generally subparallel and their continuity can be followed for about 25 – 30 kilometers. These marine sedimentary deposits seems to be syn-tectonic to the normal faulting and subduction of the Rivera Plate. Their deformation is mainly characterized by thrusts and reverse faults mostly with west vergence, although some of them have east vergence as well. The sedimentary sequence can be divided into four subunits delimited by their geometric relationships, presenting onlap, downlap and erosive truncations geometries (Fig. 18). This geometry would indicate different phases of sedimentation during the subduction of the Rivera plate, difficult to date due to a lack of information of wells, drills or cores in this unexplored area.

The accretionary prism is formed by a thick sedimentary succession (up to 4 seconds TWTT of maximum thickness) characterized by a set of reflectors with a lack of lateral continuity, being mostly formed by chaotic facies (see Figure 16 and 17). This is probably due to the high deformation activity to which the sediments are liable to.

The basement of the accretionary prism presents a very sharp paleo-relief, and two basins have been identified (Fig. 19). The western slope

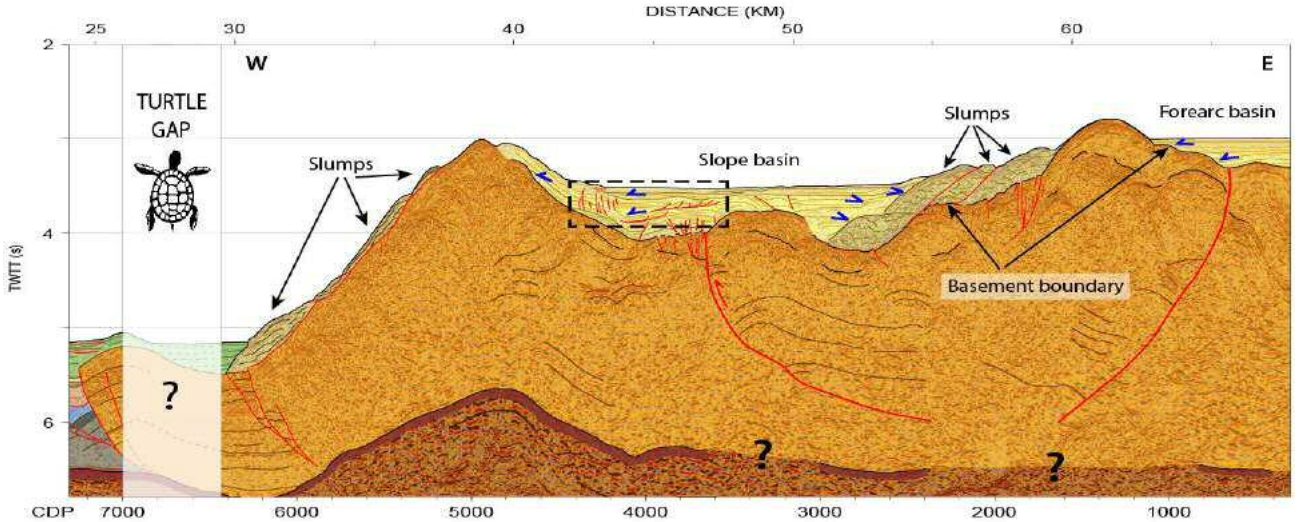

Fig. 19 – Accretionary prism of the subduction system, and the slope and forearc basins can be observed and interpreted in profile TS06b. Basins present onlap (blue arrows) geometry. The dashed box indicates extensional gravitational collapse and the resultant thrusts formation.

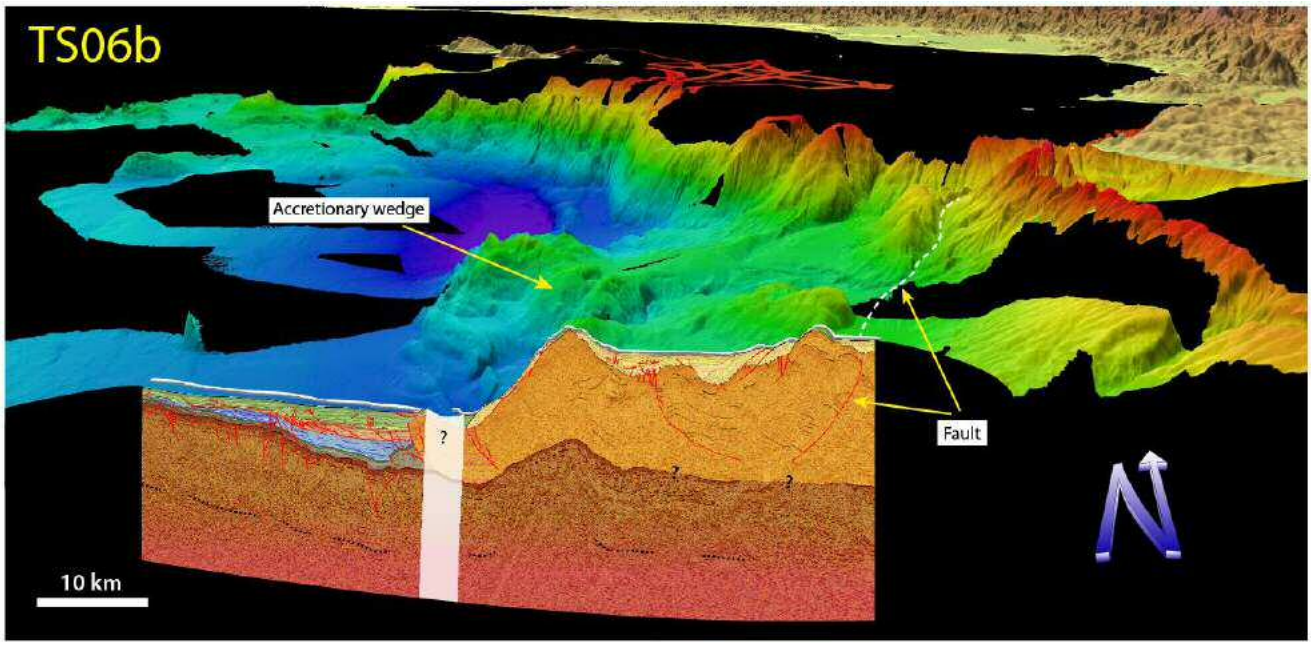

Fig. 20 – Location of the line TS06b in the 3-D high-resolution bathymetry data, which mapped the seafloor of the western Mexican margin during the survey. A fault observed in the bathymetry is interpreted in the seismic line.

basin, located in the center of the accretionary prism (between CDP 1600 to CDP 4800), and the sediments observed may be originated during the erosion of the accretionary prism. This took place during different episodes of uplift, generating slumps and normal faults related to gravitational movements that give rise to thrusts in the upper block (see figure 19). The second basin, located on the eastern border of the profile (from CDP 1 to CDP 1200), is the forearc basin of the subduction system, whose sediments are onlaping the basement. Also a system of slumps that reaches the base of the prism has been observed (from CDP 5000 to CDP 6400), covered by marine sediment units.

Three major fracture zones can be identified in the accretionary wedge. The first one, located in the westernmost part (about CDP 7200), presents west vergence and constitutes the frontal thrust of the prism, being the boundary between the accretion prism and the marine sediments covering the Rivera plate, and possibly caused by the accretion process (see figure 17). The second fractured zone located in the center of the accretionary prism (around CDP 3600) has been interpreted as a thrust, with a west dipping orientation, which actually crosses the top of the basement. The last major fracture is located in the eastern part of the profile at 65 km (about CDP 600). This is a fault not observed in the seismic profile but it has been identified through the 3-D high-resolution bathymetry data, acquired for the period of the survey during the seafloor ocean mapping along the margin (Fig. 20). High-resolution swath-bathymetry data was acquired with two Kongsberg Simrad's multibeam echosounders, hull-mounted in the vessel RSS James Cook.

5.2 Presence of hydrated gas

A significant presence of hydrocarbon as gas hydrates, identified as BSR reflectors in seismic records, has been recognized in the accretionary wedge and forearc basin at 0.25 – 0.3 seconds (TWTT) below the seafloor and extends for about 25 km along the profile (from CDP 5800 to CDP

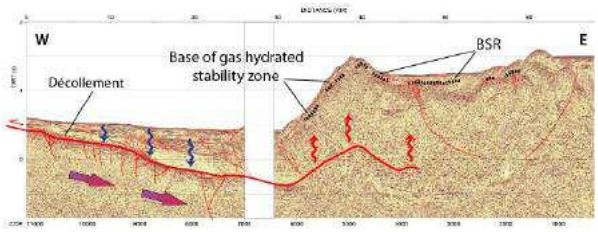

Fig. 21 – Structural interpretation of the line TS06b, from 2 seconds to 8 seconds TWTT, illustrating the transfer of fluids and the formation of the gas hydrates along the décollement.

2200) . Most of the reflection amplitude of the BSR is caused by the underlying free gas, which its formation is dominated by hydrate recycling in subduction zone accretionary wedge. The base of the zone in which hydrate can exist is limited by the increase in temperature and pressure with depth beneath the seabed. In some cases, BSR is disrupted by the presence of faulting. When faulting occurs, BSR reflector is difficult to be observed as gas hydrates may scape and the impedance contrast disappears (Fig. 21).

6 DISCUSSION OF RESULTS

Processing and geological interpretation of the line TS06b has allowed to obtain, for the first time, a seismic image of the subduction zone of the Rivera plate beneath North American plate. The work made involves a detail knowledge of the main structures in the area at crustal scale, which have been characterized by their geometry, morphology, dimension, deformation and fracturing of the internal structure, including the depth at which they are located and their lateral continuity. In this way, accretionary prism, slope basins associated, forearc basin, crust - mantle boundary and interplate limit have been identified. As a result, the structural and geometrical information provided by this profile constitute an essential contribution to understand the geodynamic context of the area and also provide a baseline for future works and projects in the area.

Most of the reflection amplitude of the BSR, which identifies the presence of gas hydrates in the accretionary prism and continental slope, are visible and can be observed. The purpose of this work, seismic processing and interpretation of this MCS profile, is to visualize large structures in depth. So to get a better definition of these anomalous reflectors would be necessary to apply some specific fine-tuning steps, such as frequency wave number filtering, CMP-consistent statics and surface-consistent scaling and residual statics.

Deep faulting observed along the profile and the identification of gas hydrates in the accretionary prism, may imply a particulary important role of circulation of fluids in a particular two areas.In the décollement zone or basal thrust, which acts as a conduit for fluids producing wet sediments, and in the accretionary wedge, where there are rapid rates of upward fluid flow and seafloor uplift (Fossen, 2010) (see figure 21). Therefore, it is more likely to occur serpentinization processes in this zone. Serpentinization is the alteration process of olivine in the presence of water. In subduction zones this process occurs along deep faults where oceanic plates enter into subduction, near the base of the mantle wedge at depths greater than 10 km (Manea et al., 2011) and up to 150 meters depth. The décollement or basal thrust is identified in the interplate boundary, but the seismogenic zone is located in deeper areas of the subduction system, East of profile TS06b. Subduction of serpentinized fracture zones enhances the generation of earthquakes and melting production in the mantle wedge, being able to influence the position of the melting front.

A future application of the results of this work is to perform a thermal modeling of the subduction zone. In order to constrain the model, a value of sediment thickness is critical. Sediment thickness

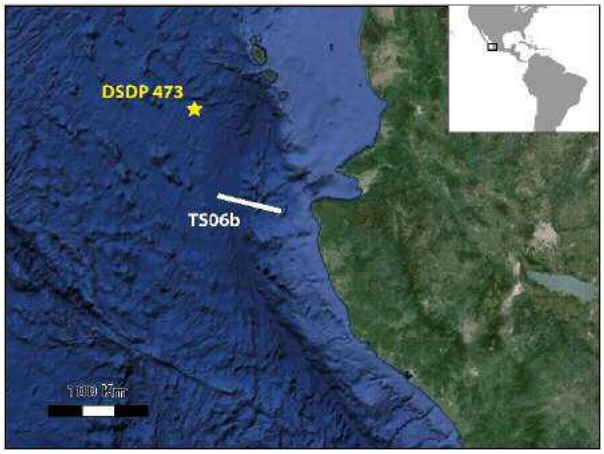

Fig. 22 – Location of site 473 and line TS06b.

measured in two-way travel time along the profile, could be estimated in depth from the velocity stack model obtained during the processing of line TS06b, previously converted to interval velocities.

The Deep Sea Drilling Project (DSDP) was the first of three international scientific ocean drilling programs that have operated around the world over more than 40 years. One of the ocean boreholes, site 473, was drilled to 287.5 meters on November 22, 1978 at the mouth of the Gulf of California, a close location to the position of the line TS06b (Fig. 22).

Site 473 was cored continuously to obtain an upper Neogene reference section to investigate the possibility that oceanic crust at the mouth of the gulf formed prior to 4 M.y. ago. Terrigenous clay that was deposited from the early Pliocene to the Quaternary, locally containing silt or ash, was cored to 143 meters, and moderately indurated diatomaceous and calcareous claystone deposited in the early Pliocene was cored from 143 to 181 meters. The boundary between these two sub-units, identified mainly on the basis of the difference in consolidation, is a seismic reflector. From 181 meters to the base of the sedimentary section at 248.1 meters, silty claystone and local silty quartzose sand, deposited in the late Miocene and early Pliocene, include turbidites with common Bouma T_c, T_d and T_c, T_d, and T_e sequences. The age of the basal sediments is 6 to 7 M.y. old. Sediment velocities are 1.5 to 1.6 km/s from mudline to 181 meters, increasing to 1.98 km/s at the basal sediments. Igneous rocks below the sediments are mainly massive, altered diabase with a density of 2.7 g/cm3 and a velocity of 5.2 to 5.3 km/s, but a fragment of pillow basalt was found at the bottom of the core (Fig. 23).

Due to the position of the site 473 with respect to the line, we cannot directly correlate the materials of borehole with materials of line TS06b. However, this information may help to know or infer the type of materials and sedimentary facies that could characterize to marine deposits located in the western part of the line TS06b, as a future work.

7 CONCLUSIONS

The western margin of Mexico is a region with the interaction of several tectonic plates so for this reason is considered one of the most active seismic zone in America, and the earthquakes and

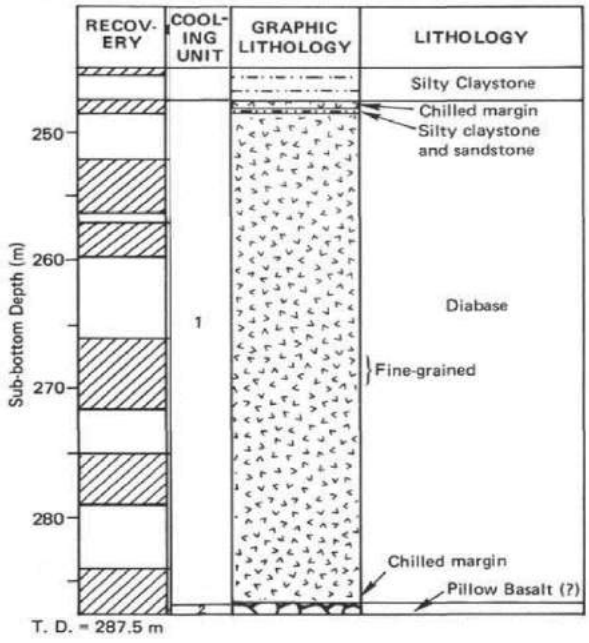

Fig. 23 – Synthetic sedimentary sequence at 473 site (Image obtained from DSDP Volume LXIII)

tsunamis generation suppose a great risk, especially in coastal. This work has been tried to characterize the geological features of the Rivera plate subduction zone from line TS06b of the TSUJAL survey.

The seismic processing that I have applied to the line TS06b mainly included, in order of application, the editing, deconvolution, CDP sorting, NMO correction, stack and migration process, applying several filters and complementary processes along the workflow. The objective of this processing was focused on obtaining the best image at crustal scale so it has allowed to characterize the internal structure of the Rivera plate subduction zone, being able to appreciate some of the local details.

The multichannel seismic marine data acquired in the line TS06b of the TSUJAL survey and its subsequent processing and geological interpretation has allowed to obtain for the first time a suitable seismic image of the subduction zone of the Rivera plate beneath the North American plate. The lack of detailed information previous to this work about subduction zone of the Rivera plate, make it into a relevant work for the performance of future work or projects on the area.

To know the seismogenic activity of the faults identified in subduction zone in order to predict the possible generation of tsunamis, it is necessary to collect more data in the area, both geophysical and geological as well as performing ocean drilling of deep and coring in order to date the reflectors and configure a geodynamic history of the margin.

The completion of this work has allowed me to acquire knowledge on techniques of seismic processing, also useful for hydrocarbon exploration, and to know how to deal with complex situations and problems relating to the compilation, analysis and interpretation of geophysical and geological data.

8 ACKNOWLEDGEMENTS

Especially to my supervisors, David Martí and Rafael Bartolomé, for the confidence that they have placed on me to develop this work, for their patience and cooperation, and for teaching me the necessary basis to carry out a project of this characteristics. Thank you both them for giving me the opportunity to do this work.

Thanks to Alejandra Lago and Marina Viñas, interns of the Institute of Marine Sciences in Barcelona, for helping me in my rookie questions. Especially Alejandra, for all the hours spent with me in the last months of her PhD thesis.

9 REFERENCES

Allan, J. F. (1986). Geology of the northern Colima and Zacoalco grabens, southwest Mexico: Late Cenozoic rifting in the Mexican Volcanic Belt. *Geological Society of America Bulletin*, *97*(4), 473-485.

Bandy, W. L., Hilde, T. W. C., & Yan, C. Y. (2000). The Rivera-Cocos plate boundary: Implications for Rivera-Cocos relative motion and plate fragmentation. *Geological Society of America Special Papers*, *334*, 1-28.

Bartolomé, R. *Evolución tectónica del margen continental oeste de Mexico: Fosa Mesoamericana y Golfo de California (CORTES-P96).(2002)* (Doctoral dissertation, Tesis Doctoral, Universidad de Barcelona).

Bartolomé, R. (2014). TSUJAL Marine Cruise Report.

DeMets, C., & Stein, S. (1990). Present-day kinematics of the Rivera Plate and

implications for tectonics in southwestern Mexico. *Journal of Geophysical Research: Solid Earth (1978–2012)*, *95*(B13), 21931-21948.

DeMets, C., Jansma, P. E., Mattioli, G. S., Dixon, T. H., Farina, F., Bilham, R. & Mann, P. (2000). GPS geodetic constraints on Caribbean-North America plate motion. *Geophys. Res. Lett*, *27*(3), 437-440.

Dougherty, S. L., Clayton, R. W., & Helmberger, D. V. (2012). Seismic structure in central Mexico: Implications for fragmentation of the subducted Cocos plate. *Journal of Geophysical Research: Solid Earth (1978–2012)*,*117*(B9).

Eissler, H. K., & McNally, K. C. (1984). Seismicity and tectonics of the Rivera plate and implications for the 1932 Jalisco, Mexico, earthquake. *Journal of Geophysical Research: Solid Earth (1978–2012)*, *89*(B6), 4520-4530.

Farreras, S. A. L. V. A. D. O. R. (1997). Tsunamis en México. *LAVIN, MF Contribuciones a la Oceanografía Física en México. Ciudad de México: Unión Geofísica Mexicana, Monografía*, (3), 73-96.

Fossen, H. (2010). *Structural geology*. Cambridge University Press.

Haacke, R. R., Westbrook, G. K., & Hyndman, R. D. (2007). Gas hydrate, fluid flow and free gas: Formation of the bottom-simulating reflector. *Earth and Planetary Science Letters*, *261*(3), 407-420.

Johnson, C. A., & Harrison, C. G. A. (1989). Tectonics and volcanism in central Mexico: a Landsat thematic mapper perspective. *Remote Sensing of Environment*, *28*, 273-286.

Lonsdale, P. (1989). Geology and tectonic history of the Gulf of California. *The eastern Pacific Ocean and Hawaii: Boulder, Colorado, Geological Society of America, Geology of North America, v. N*, 499-521.

Manea, V. C., & Manea, M. (2011). Flat-slab thermal structure and evolution beneath central Mexico. *Pure and Applied Geophysics*, *168*(8-9), 1475-1487.

Minshull, T. A., Bartolomé, R., Byrne, S., & Danobeitia, J. (2005). Low heat flow from young oceanic lithosphere at the Middle America Trench off Mexico.*Earth and Planetary Science Letters*, *239*(1), 33-41.

Pardo, M., & Suarez, G. (1995). Shape of the subducted Rivera and Cocos plates in southern Mexico: Seismic and tectonic implications. *Journal of Geophysical Research: Solid Earth (1978–2012)*, *100*(B7), 12357-12373.

Resnick, J. R. (1993). Seismic data processing for AVO and AVA analysis.*Offset-dependent reflectivity: Theory and practice of AVO analysis: Society of Exploration Geophysicists, Investigations in Geophysics Series*, *8*, 175-188.

Singh, S. K. Ponee, L. Nishenko, S. P. (1985). The great Jalisco, Mexico, earthquakes of 1932: subduction of the Rivera plate, Bull. Seism. Soc. Am. **75**,1301- 1314.

Suárez, G., García-Acosta, V., & Gaulon, R. (1994). Active crustal deformation in the Jalisco block, Mexico: evidence for a great

historical earthquake in the 16th century. *Tectonophysics*, *234*(1), 117-127.

Yilmaz, Ö. (2001). *Seismic data analysis* (Vol. 1, pp. 74170-2740). Tulsa, OK: Society of exploration geophysicists.